

Crystalline Mo_3VO_x Mixed-Metal-Oxide Catalyst with Trigonal Symmetry**

Masahiro Sadakane,* Nobufumi Watanabe, Tomokazu Katou, Yoshinobu Nodasaka, and Wataru Ueda*

About a quarter of all organic products are synthesized by selective partial oxidation and continuous efforts have been made to develop high-performance catalysts that improve conversion and selectivity. The majority of catalysts are metal oxides with either molybdenum or vanadium as one of the key elements.^[1] Recently, much attention has been paid to orthorhombic MoVTe(Sb)NbO mixed-metal-oxide catalysts developed by Mitsubishi Chemicals, which have the best performance in propane oxidation to acrylic acid and ammoxidation to acrylonitrile.^[2] Although a fully analyzed crystal structure of the catalyst has not yet been reported, it was shown that this complex mixed-metal oxide has a layered, orthorhombic structure with a slab comprising 6- and 7-rings of $\{\text{MO}_6\}$ octahedra and pentagonal $\{\text{(M)}\text{M}_5\text{O}_{27}\}$ units with a $\{\text{MO}_7\}$ pentagonal bipyramidal unit and five edge-sharing $\{\text{MO}_6\}$ octahedra (M is a metal atom; Figure 1 a).^[3]

In the course of our investigation to design a catalyst for selective oxidation, we succeeded in synthesizing an orthorhombic mixed-metal oxide that contains Mo and V atoms, with and without other elements (Te, Sb, or Nb) under hydrothermal conditions.^[4] Herein, we describe the synthesis and structural characterization of a novel crystalline Mo_3VO_x mixed-metal oxide (trigonal, Figure 1 b $x \leq 11.1$), which contains the same building units (6- and 7-rings and a pentagonal unit) as orthorhombic Mo_3VO_x but in different ratios. Like

orthorhombic Mo_3VO_x , trigonal Mo_3VO_x showed outstanding catalytic activity for the selective oxidation of acrolein, which indicates the importance of these structures for this catalytic activity.

Both orthorhombic and trigonal Mo_3VO_x mixed-metal oxides were synthesized from a reaction mixture of ammonium heptamolybdate, $(\text{NH}_4)_6\text{Mo}_7\text{O}_{24} \cdot 4\text{H}_2\text{O}$, and vanadyl sulfate, $\text{VOSO}_4 \cdot n\text{H}_2\text{O}$ ($\text{Mo}:\text{V} = 4:1$), in H_2O under hydrothermal conditions. By controlling the pH value of the precursor solution, the orthorhombic or trigonal Mo_3VO_x was selectively synthesized (Scheme 1). The crude materials contained amorphous phase as a by-product, which was removed by washing the products with aqueous oxalic acid. The ratio of Mo:V atoms was determined by inductively coupled plasma atomic emission spectroscopy (ICP-AES) and was about 3:1 for both materials.

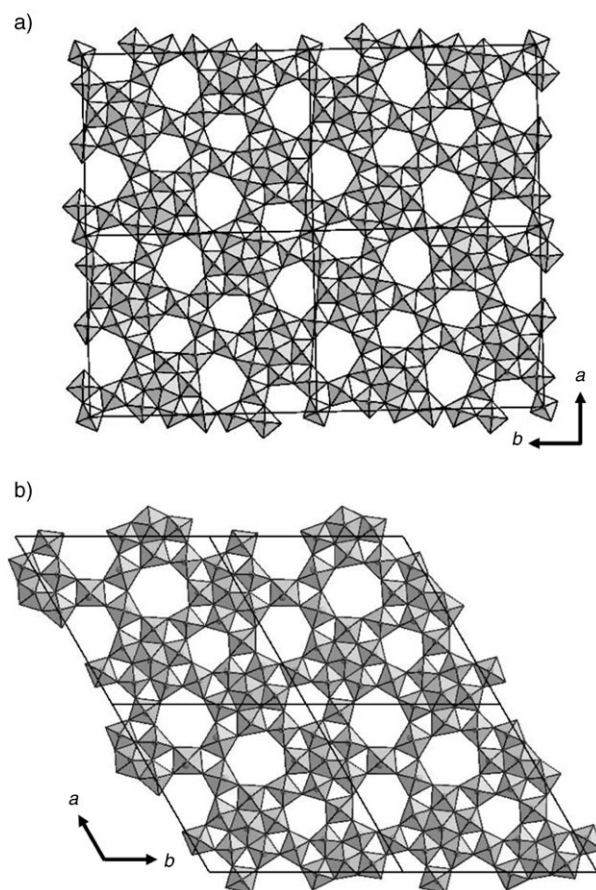


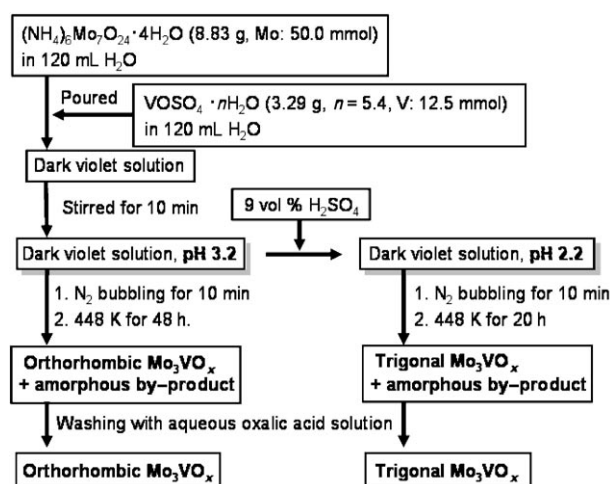
Figure 1. Polyhedral presentation of the structures of a) orthorhombic and b) trigonal Mo_3VO_x . (The basic structure of MoVTe(Sb)NbO is the same as Mo_3VO_x .)

[*] Dr. M. Sadakane, N. Watanabe, T. Katou, Prof. W. Ueda
Catalysis Research Center
Hokkaido University
N-21, W-10, Sapporo, 001-0021 (Japan)
Fax: (+81) 11-706-9164
E-mail: sadakane@cat.hokudai.ac.jp
ueda@cat.hokudai.ac.jp

Y. Nodasaka
Laboratory of Electron Microscopy
Graduate School of Dental Medicine
Hokkaido University
Sapporo (Japan)

[**] Supported in part by Grants-in-Aid for Scientific Research "B" (No: 16360396), "Grant for Research" of The Japan Petroleum Institute, and "Nanotechnology Support Project" of the Ministry of Education, Culture, Sports, Science and Technology (MEXT), Japan. We thank Dr. T. Nagai, Dr. Y. Matsui (High Voltage Electron Microscopy Station, National Institute for Materials Science), K. Sugawara, and Prof. N. Sakaguchi (High Voltage Electron Microscope Laboratory, Center for Advanced Research of Energy Conversion Materials, Hokkaido University) for supporting TEM measurements and Nippon Kayaku Corp. for ICP-AES analysis and acrolein oxidation test.

Supporting information for this article is available on the WWW under <http://www.angewandte.org> or from the author.



Scheme 1. Synthesis of orthorhombic and trigonal Mo_3VO_x .

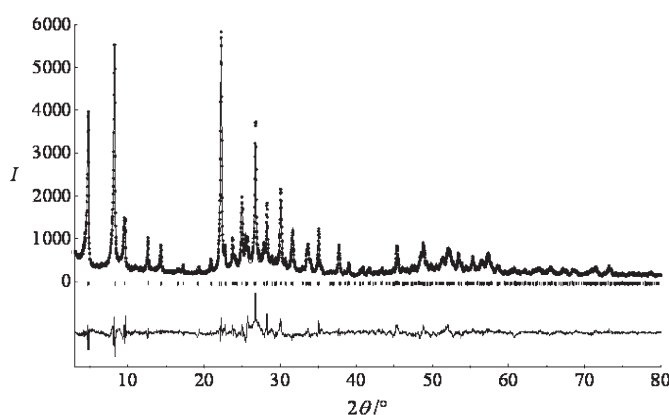


Figure 2. Observed (dots), calculated (solid line), and difference pattern (solid line, bottom) from the Rietveld analysis of the XRD data for trigonal Mo_3VO_x at room temperature, space group $P3$. Bragg reflections are indicated by tick marks.

Indexing the Bragg reflections of the powder X-ray diffraction (XRD) pattern (Figure 2) of trigonal Mo_3VO_x revealed lattice parameters of $a \approx b \approx 21 \text{ \AA}$, $c \approx 4 \text{ \AA}$, $\alpha = \beta = 90^\circ$, and $\gamma = 120^\circ$. Similar to orthorhombic Mo_3VO_x , trigonal Mo_3VO_x has a layered structure with a repetition along the c axis of 4.0 \AA , which corresponds to the M–O–M separation. It is evident from TEM and SEM observations that the a – b planes are oriented perpendicular to the long axis of the rodlike crystal, which coincides with the c direction (Figure S1 in the Supporting Information).

The trigonal structure was resolved by comparing its high-resolution (HR) TEM image with that of orthorhombic Mo_3VO_x . Figure 3 shows HRTEM images along the $[001]$ zone axis of both materials. Two kinds of white spots are present, large (L) and small (S; Figure 3). In the case of orthorhombic Mo_3VO_x , the large spots correspond to 7-rings and the small spots correspond to 6-rings of octahedral $\{\text{Mo}_6\}$ units (Figure S2 in the Supporting Information). The pentagonal rings are surrounded by three 7- and two 6-rings. The structure of trigonal Mo_3VO_x is assumed to be the same. Although the spots are slightly uneven because of a small misorientation of the crystal with respect to the incident

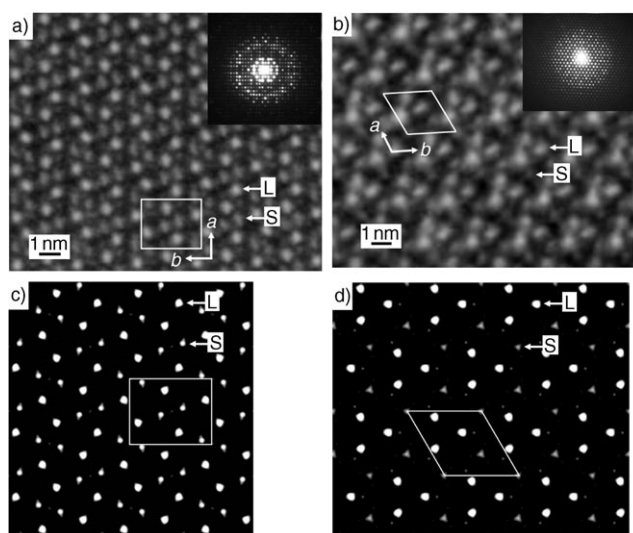


Figure 3. HRTEM images and selected-area electron diffraction (SAED) patterns (insets) of a) orthorhombic and b) trigonal Mo_3VO_x viewed along the $[001]$ direction as well as the corresponding simulated contrast for c) orthorhombic Mo_3VO_x calculated for a crystal thickness close to 24 nm and a defocus value $\Delta f = -130 \text{ nm}$ and d) trigonal Mo_3VO_x calculated for a crystal thickness close to 20 nm and a defocus value $\Delta f = -155 \text{ nm}$. L and S indicate large and small spots, respectively.

electron beam, three large white spots that correspond to a 7-ring and two small spots that correspond to a 6-ring were found per unit cell (Figure 3b). The pentagonal unit is surrounded by three 7- and two 6-rings to produce the structure presented in Figure 1b.

This trigonal structure was confirmed by analyzing the powder XRD data by the Rietveld method. Its XRD pattern (Figure 2) was simulated with lattice parameters $a = 21.433(3)$, $c = 4.0045(18) \text{ \AA}$, space group $P3$ (No. 143), which converged reasonably ($R_{wp} = 0.1223$) although Rietveld refinement with other deduced models did not converge.^[5] From these data, there is no doubt that the proposed structure is reasonable.

Orthorhombic and trigonal Mo_3VO_x were synthesized by mixing a solution of ammonium heptamolybdate with vanadyl sulfate under hydrothermal conditions to give a dark-violet solution. To elucidate the synthesis mechanism, Raman spectra of the precursor solution before the hydrothermal reaction (Figure 4, top, curves a and b) were compared with those of various polyoxomolybdate solutions. The characteristic Raman peaks at 1000 – 700 cm^{-1} are very similar to those of the polyoxomolybdates that contain the pentagonal $\{(\text{Mo})\text{Mo}_5\}$ unit; those are $\text{Mo}_{72}\text{V}_{30}$,^[6] Mo_{132} ,^[7] and Mo_{57}V_6 ,^[8] shown in Figure 4, curves c, e, and d, respectively.

The UV/Vis spectrum of the precursor solution is similar to that of $\text{Mo}_{72}\text{V}_{30}$ (Figure 4, bottom) and a band arising from intervalence charge transfer (IVCT; $\text{V}^{\text{IV}} \rightarrow \text{Mo}^{\text{VI}}$)^[6] at around 510 nm is present in both spectra. The $\text{Mo}_{72}\text{V}_{30}$ polyoxomolybdate has 12 pentagonal $\{(\text{Mo}^{\text{VI}})\text{Mo}^{\text{VI}}_5\}$ units connected by 30 vanadium(IV) centers.^[6] These results indicate that the pentagonal $\{(\text{Mo})\text{Mo}_5\}$ unit is present in the precursor solution before the hydrothermal reaction takes place. The

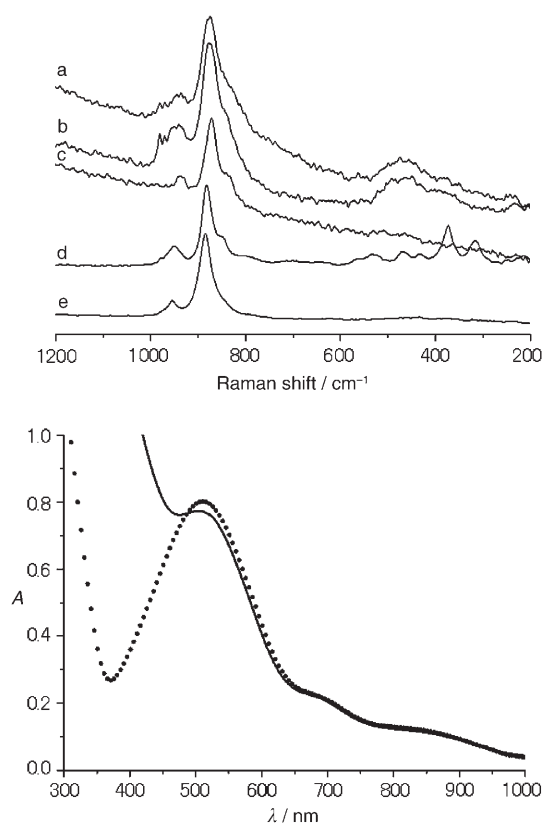


Figure 4. Top: Raman spectra of Mo–V solutions. a) Mo:V = 4:1, $c_{\text{Mo}} = 0.21$ M, pH 3.3; b) Mo:V = 4:1, $c_{\text{Mo}} = 0.21$ M, pH 2.2; c) aqueous $\text{Mo}_{72}\text{V}_{30}$ (1 g per 30 mL); d) aqueous Mo_{57}V_6 solution (1 g per 30 mL); e) aqueous Mo_{132} solution (1 g per 30 mL). Bottom: UV/Vis spectra of an Mo–V solution (Mo:V = 4:1, $c_{\text{Mo}} = 0.42$ M, pH 3.3; solid line) and an aqueous $\text{Mo}_{72}\text{V}_{30}$ solution (dotted line).

reaction of the pentagonal unit with other molybdenum and vanadium species produces orthorhombic or trigonal Mo_3VO_x depending on the pH value. The pH value is known to be one of the most important factors in producing a giant polyoxomolybdate.^[9] These discrete polyoxomolybdate units have been prepared at temperatures ranging from room temperature to 363 K by the reaction of pentagonal units with molybdenum and other metal oxides.^[9] Under hydrothermal conditions, the pentagonal unit assembled further into a complex mixed-metal oxide.

As summarized in Table 1, the trigonal Mo_3VO_x catalyst has outstanding catalytic activity for the oxidation of acrolein into acrylic acid, with a conversion of around 100 % at 463 K and selectivity to acrylic acid of 90 % (yield 90 %). The orthorhombic Mo_3VO_x catalyst shows similarly high catalytic activity. This oxidation is known as the second process in acrylic acid production. Acrylic acid (3 000 000 tons per year, worldwide) is manufactured by catalytic oxidation in a two-step process, which involves the oxidation of propene to acrolein and then to acrylic acid. The catalytic activities of our catalysts are significantly higher than those of Mo–V-based oxide catalysts reported in patents and papers, which need higher temperatures (usually more than 500 K) to obtain similar activity.^[10] These results indicate that the layered structure comprising 6- and 7-rings of metal-oxide octahedra

Table 1: Oxidation of acrolein over Mo_3VO_x catalysts to acrylic acid (AA), acetic acid (AcA), and CO/CO_2 .^[a]

Catalyst	BET Surface area [m^2g^{-1}]	Conversion [%]	Selectivity [%]		
			AA	AcA	CO/CO_2
trigonal Mo_3VO_x	15.6	99.7	90.5	3.2	6.3
orthogonal Mo_3VO_x	14.9	99.4	93.6	1.5	4.9

[a] Reaction conditions: 0.45 g of catalyst with 0.05 g of SiC; gas composition: acrolein/ O_2 / H_2O / $\text{N}_2 = 4.8/7.6/26.9/60.6$; total flow: 103.3 mL min^{-1} , reaction temperature: 463 K. Both catalysts were calcined at 673 K under a nitrogen flow before the reaction.

and pentagonal columns is important for high oxidation activity. Moreover, crude Mo_3VO_x was less active (at 503 K: 96.4 % conversion and 94.2 % selectivity to acrylic acid;^[4e] at 523 K: 99.8 % conversion and 90.9 % selectivity to acrylic acid) than the purified material. The trigonal or orthorhombic structures of Mo_3VO_x may be the true catalytically active species in previously reported Mo–V catalysts.

Experimental Section

Materials: All chemicals were reagent-grade and used as supplied and distilled water that was made in the laboratory was used throughout.

Preparation of trigonal Mo_3VO_x : $(\text{NH}_4)_6\text{Mo}_7\text{O}_{24} \cdot 4\text{H}_2\text{O}$ (8.82 g, 50 mmol) dissolved in water (120 mL) was mixed at 298 K with $\text{VOSO}_4 \cdot n\text{H}_2\text{O}$ (3.28 g, $n = 5.4$, 12.5 mmol) dissolved in water (120 mL). The resulting solution was stirred for 10 min then transferred to a 300-mL teflon liner of a stainless-steel autoclave. The pH value of the solution was adjusted to 2.2 with dilute sulfuric acid (2 mL of concentrated sulfuric acid in 20 mL of water). The reaction mixture was purged with nitrogen for 10 min then heated at 448 K for 20 h. A gray solid (about 5 g) was isolated from the reaction mixture by filtration, washed with water, and dried at 353 K overnight. The crude trigonal Mo_3VO_x was purified by treatment with oxalic acid: dry solid (4.0 g) was added to an aqueous solution of oxalic acid (0.4 M, 100 mL) and this mixture was stirred at 333 K for 30 min. The solid was isolated from the suspension by filtration, washed with water, and dried at 353 K overnight (0.8 g).

Characterization: Powder XRD patterns were recorded on a diffractometer (Rigaku, RINT Ultima+) with $\text{CuK}\alpha$ radiation. Rietveld simulation was performed using RIETAN-2000.^[11] Surface areas were determined by the Brunauer–Emmett–Teller (BET) method. Prior to the sorption measurements, the samples were degassed under vacuum at 573 K for 2 h. ICP-AES (inductively coupled atomic absorption spectroscopy) was carried out with a VISTA-PRO apparatus (Varian). Scanning electron microscopy (SEM) was performed on a JSM-7400F (JEOL). Transmission electron microscopy (TEM) images were obtained on JEM-ARM-1300 and JEM-2000FX (JEOL) electron microscopes at Hokkaido University. Specimens were embedded in TAAB Epon 812 Resin and ultrathin sections were cut with a diamond knife. A Raman study of aqueous solutions at room temperature was performed on a System 2000R NIR FT-Raman spectrometer (PERKIN ELMER). Nd:YAG laser was used to supply 300 mW at 1064 nm.

Received: September 25, 2006

Revised: November 20, 2006

Published online: January 15, 2007

Keywords: heterogeneous catalysis · molybdenum · oxidation · polyoxometalates · vanadium

- [1] a) G. Centi, F. Cavani, F. Trifirò, *Selective Oxidation by Heterogeneous Catalysis* (Eds.: M. T. Twigg, M. S. Spencer), Kluwer Academic/Plenum Publishers, New York, **2001**; b) B. K. Hodnett, *Heterogeneous Catalytic Oxidation*, Wiley, New York, **2000**.
- [2] a) T. Ushikubo, K. Oshima, A. Kayou, T. Umezawa, K. Kiyono, I. Sawaki, Mitsubishi Chem. Corp., Patent EP 529853, **1993**; b) T. Ushikubo, Y. Koyasu, S. Wajiki, Mitsubishi Chem. Corp., Patent EP 608838, **1994**; c) T. Ushikubo, K. Oshima, A. Kayou, M. Vaarkamp, M. Hatano, *J. Catal.* **1997**, *169*, 394–396; d) H. Tsuji, Y. Koyasu, *J. Am. Chem. Soc.* **2002**, *124*, 5608–5609.
- [3] a) H. Tsuji, K. Oshima, Y. Koyasu, *Chem. Mater.* **2003**, *15*, 2112–2114; b) P. DeSanto, Jr., D. J. Buttrey, R. K. Grasselli, C. G. Lugmair, A. F. Volpe, Jr., B. H. Toby, T. Vogt, *Z. Kristallogr.* **2004**, *219*, 152–165; c) P. DeSanto, Jr., D. J. Buttrey, R. K. Grasselli, C. G. Lugmair, A. F. Volpe, B. H. Toby, T. Vogt, *Top. Catal.* **2003**, *23*, 23–38.
- [4] a) N. Watanabe, W. Ueda, *Ind. Eng. Chem. Res.* **2006**, *45*, 607–614; b) W. Ueda, D. Vitry, T. Kato, N. Watanabe, Y. Endo, *Res. Chem. Intermed.* **2006**, *32*, 217–233; c) T. Katou, D. Vitry, W. Ueda, *Catal. Today* **2004**, *91–92*, 237–240; d) D. Vitry, Y. Morikawa, J. L. Dubois, W. Ueda, *Appl. Catal. A* **2003**, *251*, 411–424; e) T. Katou, D. Vitry, W. Ueda, *Chem. Lett.* **2003**, *32*, 1028–1029.
- [5] Crystallographic parameters, agreement factors, and atomic positions are summarized in Supporting Information (Tables S1 and S2). We assumed that the pentagonal unit contains only Mo atoms and that these units are connected by V and Mo atoms for the following reasons: 1) the Raman pattern of the precursor solution was very similar to that of the $\text{Mo}_{72}\text{V}_{30}$ cluster, in which $\{(\text{Mo})\text{Mo}_5\}$ units are connected by V atoms; 2) all pentagonal units reported in polyoxometalates comprise only Mo, even in mixed polyoxomolybdates ($\text{Mo}_{72}\text{V}_{30}$, $\text{Mo}_{72}\text{Fe}_{30}$, and Mo_{57}V_6); 3) this assumption gave the best fitting result.
- [6] a) A. Müller, A. M. Todea, J. van Slageren, M. Dressel, H. Bögge, M. Schmidtman, M. Luban, L. Engelhardt, M. Rusu, *Angew. Chem.* **2005**, *117*, 3925–3929; *Angew. Chem. Int. Ed.* **2005**, *44*, 3857–3861; b) B. Botar, P. Kögerler, C. L. Hill, *Chem. Commun.* **2005**, 3138–3140.
- [7] A. Müller, E. Krichemeyer, H. Bögge, M. Schmidtman, F. Peters, *Angew. Chem.* **1998**, *110*, 3567–3571; *Angew. Chem. Int. Ed.* **1998**, *37*, 3360–3363.
- [8] A. Müller, E. Krichemeyer, S. Dillinger, H. Bögge, W. Plass, A. Proust, L. Dloczik, C. Meyer, R. Rohlfing, *Z. Anorg. Allg. Chem.* **1994**, *620*, 599–619.
- [9] Reviews: a) A. Müller, *Chem. Commun.* **2003**, 803–806; b) A. Müller, P. Kögerler, A. W. M. Dress, *Coord. Chem. Rev.* **2001**, *222*, 193–218; c) L. Cronin, P. Kogerler, A. Müller, *J. Solid State Chem.* **2000**, *152*, 57–67; d) A. Müller, C. Serain, *Acc. Chem. Res.* **2000**, *33*, 2–10; e) A. Müller, P. Kögerler, C. Kuhlmann, *Chem. Commun.* **1999**, 1347–1358.
- [10] a) H. Hibst, A. Tenten, L. Marosi (BASF Aktiengesellschaft), Patent EP 774297, **1997**; b) J. Tichý, *Appl. Catal. A* **1997**, *157*, 363–385; c) W.-h. Lee, K.-h. Kang, D.-h. Ko, Y.-c. Byun (Lg Chemical), Patent US 6171998, **2001**; d) M. Tanimoto, D. Nakamura, H. Yunoki (Nippon Shokubai Co. Ltd.), Patent EP 1106248, **2001**.
- [11] F. Izumi, T. Ikeda, *Mater. Sci. Forum* **2000**, 321–324, 198.